2016 CEDAR-GEM Workshop
June 19 – June 24, 2015

Impact of midnight thermosphere dynamics on the equatorial ionospheric vertical drifts

Tzu-Wei Fang[1,2]

R. Akmaev[2], R. Stoneback[3], T. Fuller-Rowell[1,2], H. Wang[1,2]

[1] CIRES/University of Colorado at Boulder

[2] NOAA Space Weather Prediction Center

[3] Physics Department, University of Texas at Dallas

The study is supported by NSF CEDAR Program (AGS-1243129)

Impact of MTM on the nighttime equatorial ionosphere

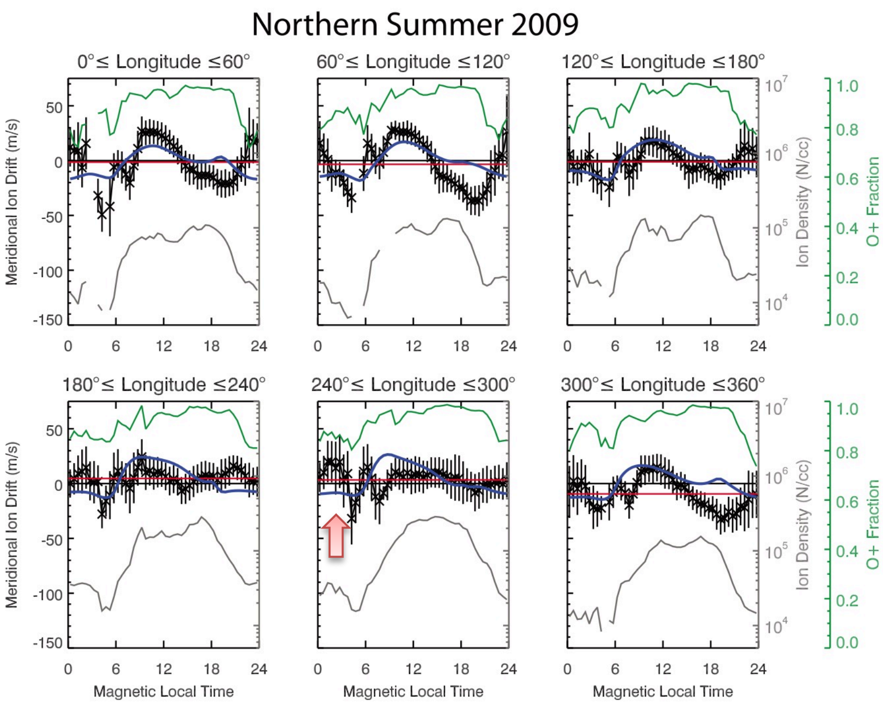

Stoneback et al. (2011)

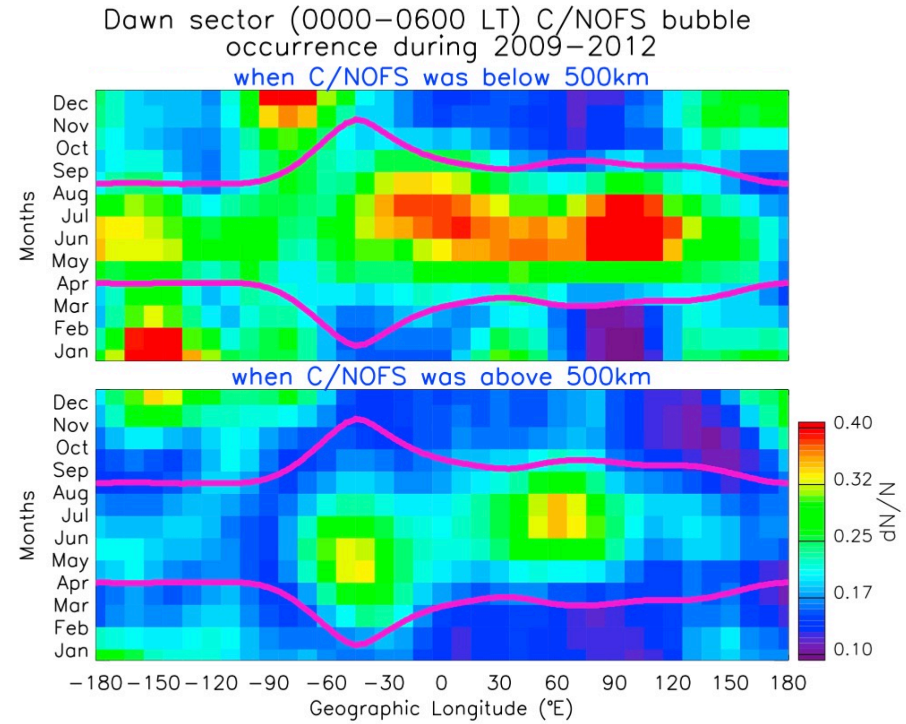

Yizengaw et al. (2013)

The C/NOFS IVM observations (left) revealed significant upward drifts during the post-midnight period. The occurrence of upward drift shows large longitudinal variation and is more pronounced near June solstice. Significant plasma bubbles after post-midnight during June solstice have also been observed by C/NOFS PLP, which may be related to the strong upward drift (right).

Midnight Temperature Maximum (MTM)

- WAM appears to be the first comprehensive model to internally generate an MTM of a realistic magnitude in the thermosphere. Simulation results from the WAM have shown the robust feature of MTM and the associated midnight density maximum (MDM).
- Model results indicate that the feature may be traced down to the lower thermosphere, where it is manifested primarily in the form of an upward propagating terdiurnal tidal wave. Thermospheric tides with higher-order zonal wavenumbers and frequencies can also contribute to the feature.

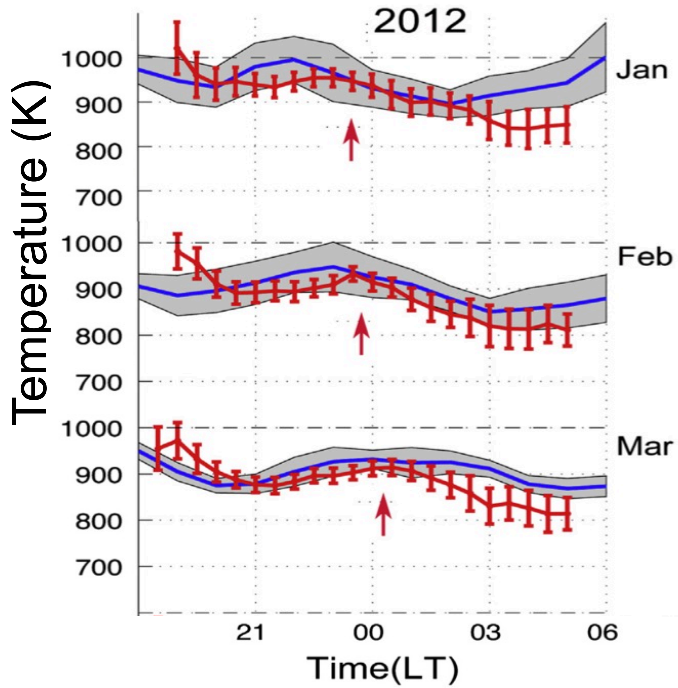

Comparisons of WAM MTM with FPI measurements at Brazil from Sep 2009 to Aug 2012 (Meriwether et al., 2013).

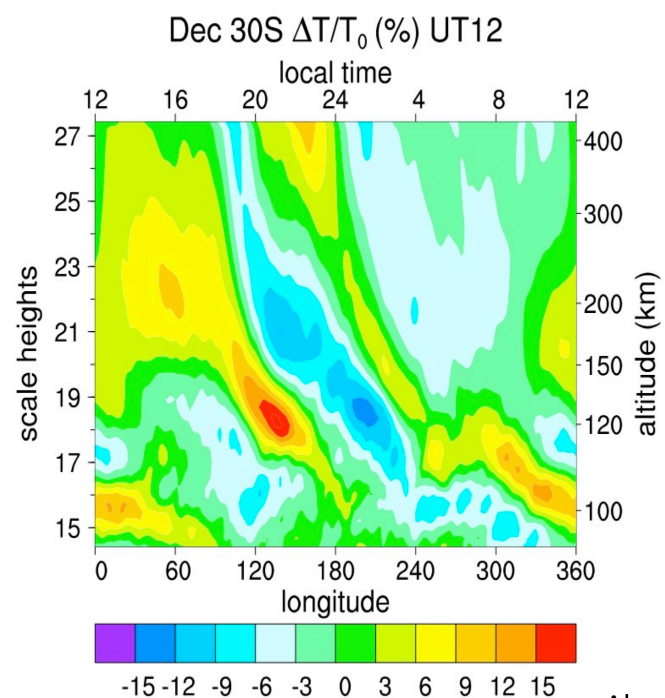

Akmaev et al. (2009)

WAM simulation of relative temperature deviation as a function of height and longitude (local time)

Midnight Temperature Maximum (MTM)

- WAM appears to be the first comprehensive model to internally generate an MTM of a realistic magnitude in the thermosphere. Simulation results from the WAM have shown the robust feature of MTM and the associated midnight density maximum (MDM).
- Model results indicate that the feature may be traced down to the lower thermosphere, where it is manifested primarily in the form of an upward propagating terdiurnal tidal wave. Thermospheric tides with higher-order zonal wavenumbers and frequencies can also contribute to the feature.

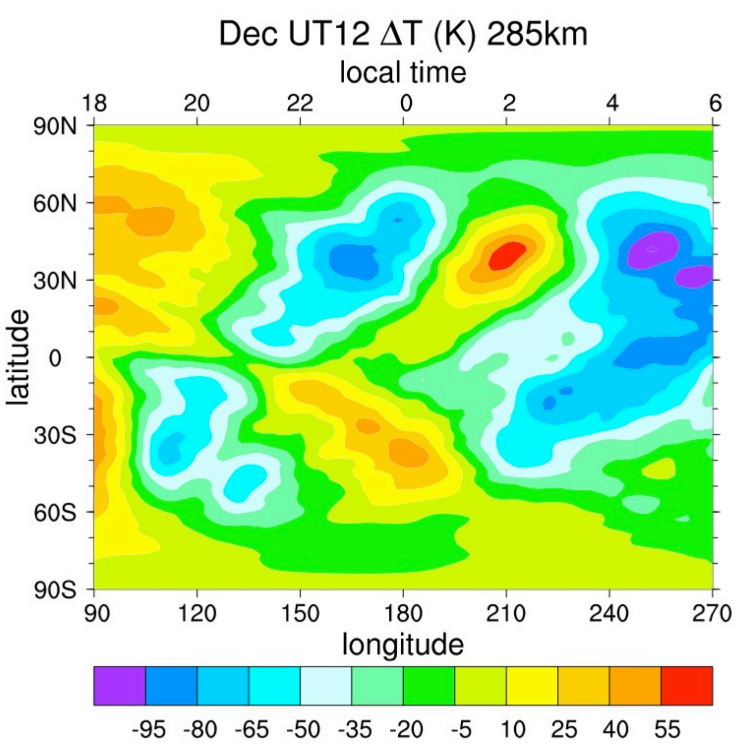

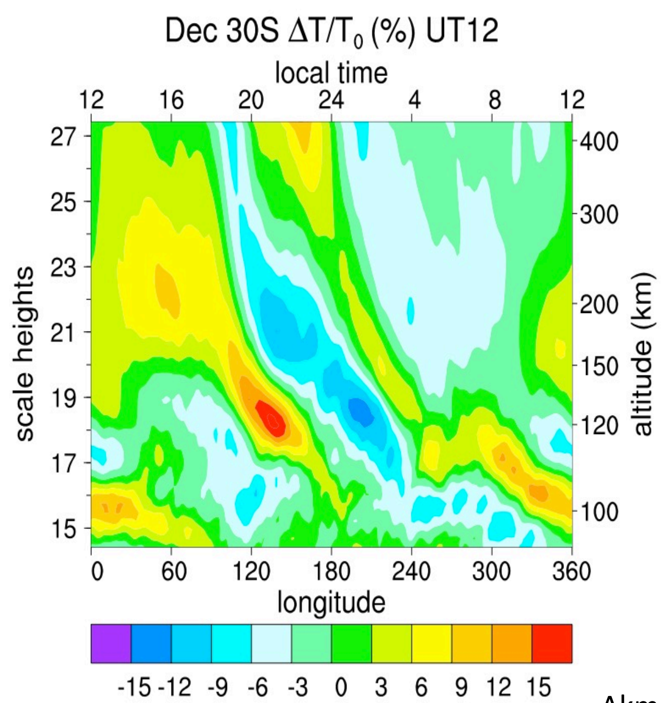

Akmaev et al. (2009)

WAM simulation of relative temperature deviation as a function of height and longitude (local time)

Whole Atmosphere Model (WAM)

- Extended Global Forecast System (GFS) upper boundary from 64 km to 600 km
- Resolution 2°×2° in latitude-longitude, H/4 in altitude
- Free or forecast runs
- Height dependent g(z)
- Orographic gravity waves parameterization
- Horizontal & vertical mixing
- Radiative heating (EUV & UV) and cooling
- Ion drag & Joule heating
- Major species composition, Eddy mixing

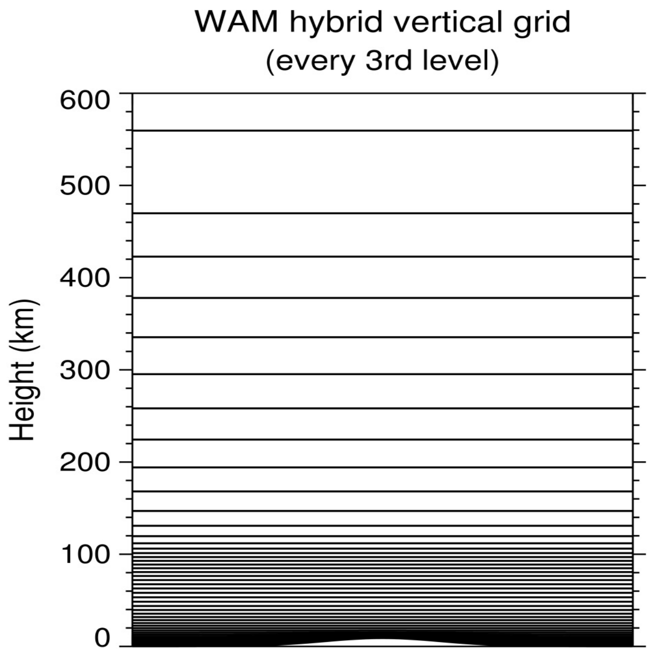

Global Ionosphere and Plasmasphere Model (GIP)

- The horizontal resolution in the low-latitude region is about 1° in latitude and 4.5° in longitude. In altitude, it covers the plasmasphere and gives information from 100 km to higher than 20,000 km.
- It solves continuity, momentum, energy equations and outputs are Ni (O^+, H^+, O_2^+, NO^+, N_2^+, N^+), Ne, Ti, Te and Vi.
- The apex coordinate system (*Richmond*, 1995) is adopted in the structure of magnetic field, in which a global three-dimensional grid are created by tracing through the full International Geomagnetic Reference Field (IGRF).

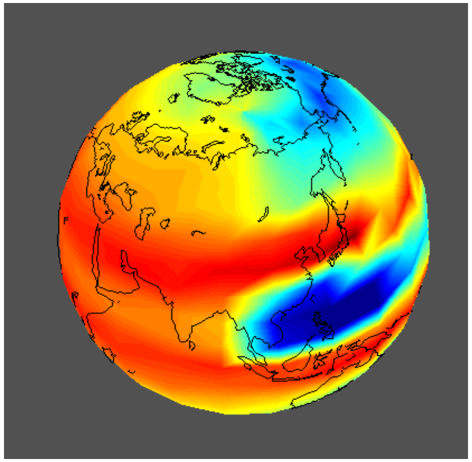

Vertical Ion Drifts from Models and Observation

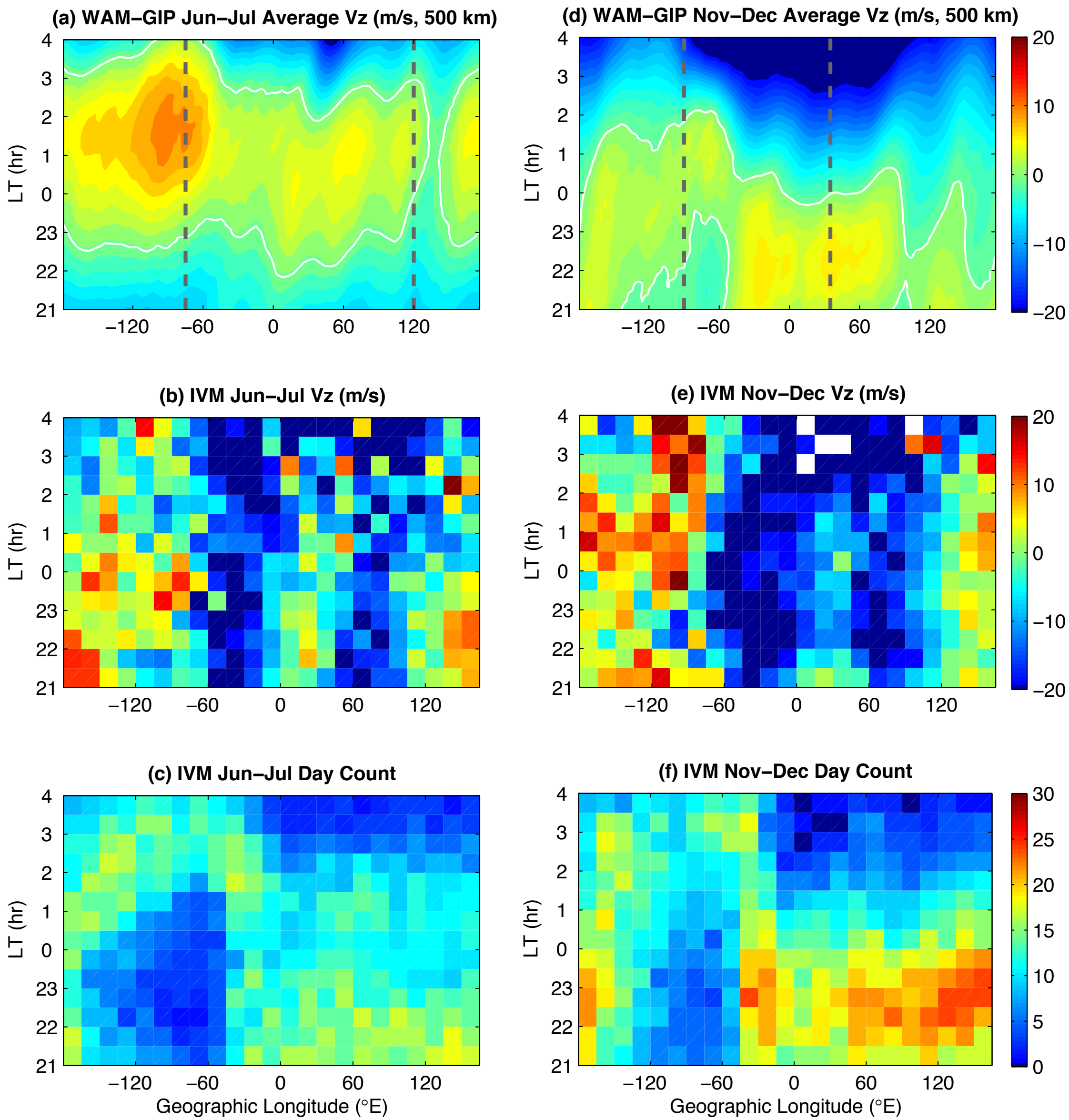

WAM-GIP climatology

C/NOFS IVM Vz climatology

C/NOFS IVM day count

June-July 2010

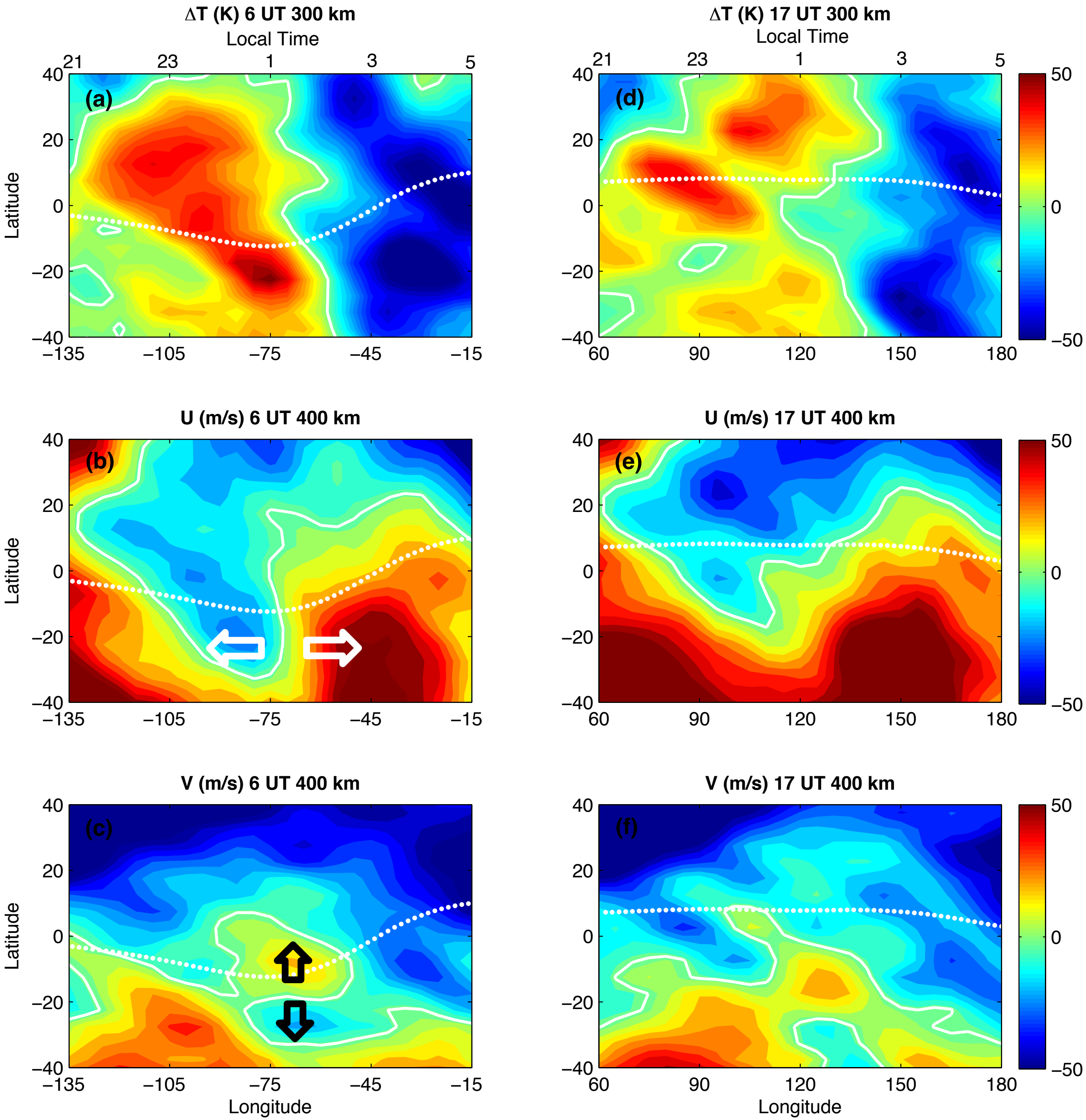

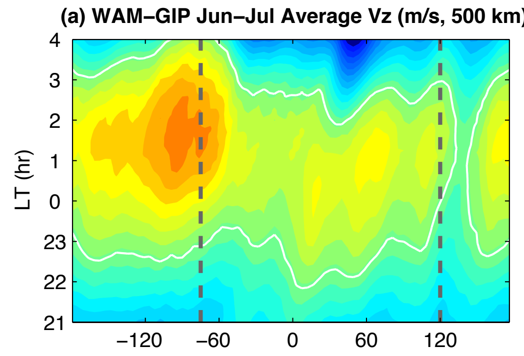

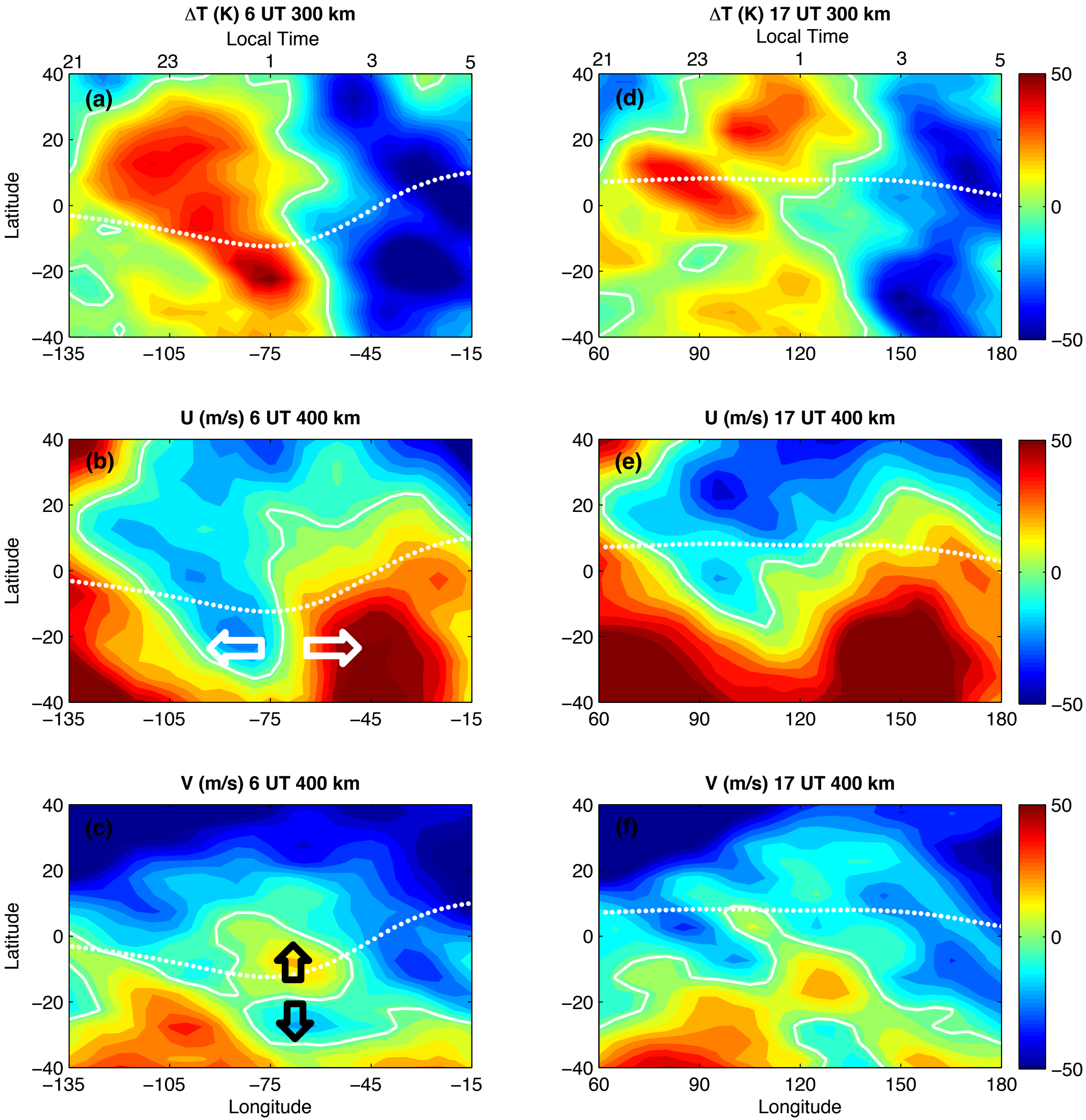

June-July 2010

- The temp maximum in the underlying layers raises the pressure at heights above resulting in a local pressure bulge. The horizontal pressure gradient drives the wind away from the pressure bulge.
- The eastward acceleration of the zonal wind across the zero wind line results in ion convection pattern similar to the conditions during the PRE and create an upward ion drift.
- The effect of the local meridional wind structures on plasma motion depends on their position with respect to the magnetic equator.
- The magnitude of the temperature peak also matters.

Nov-Dec 2010

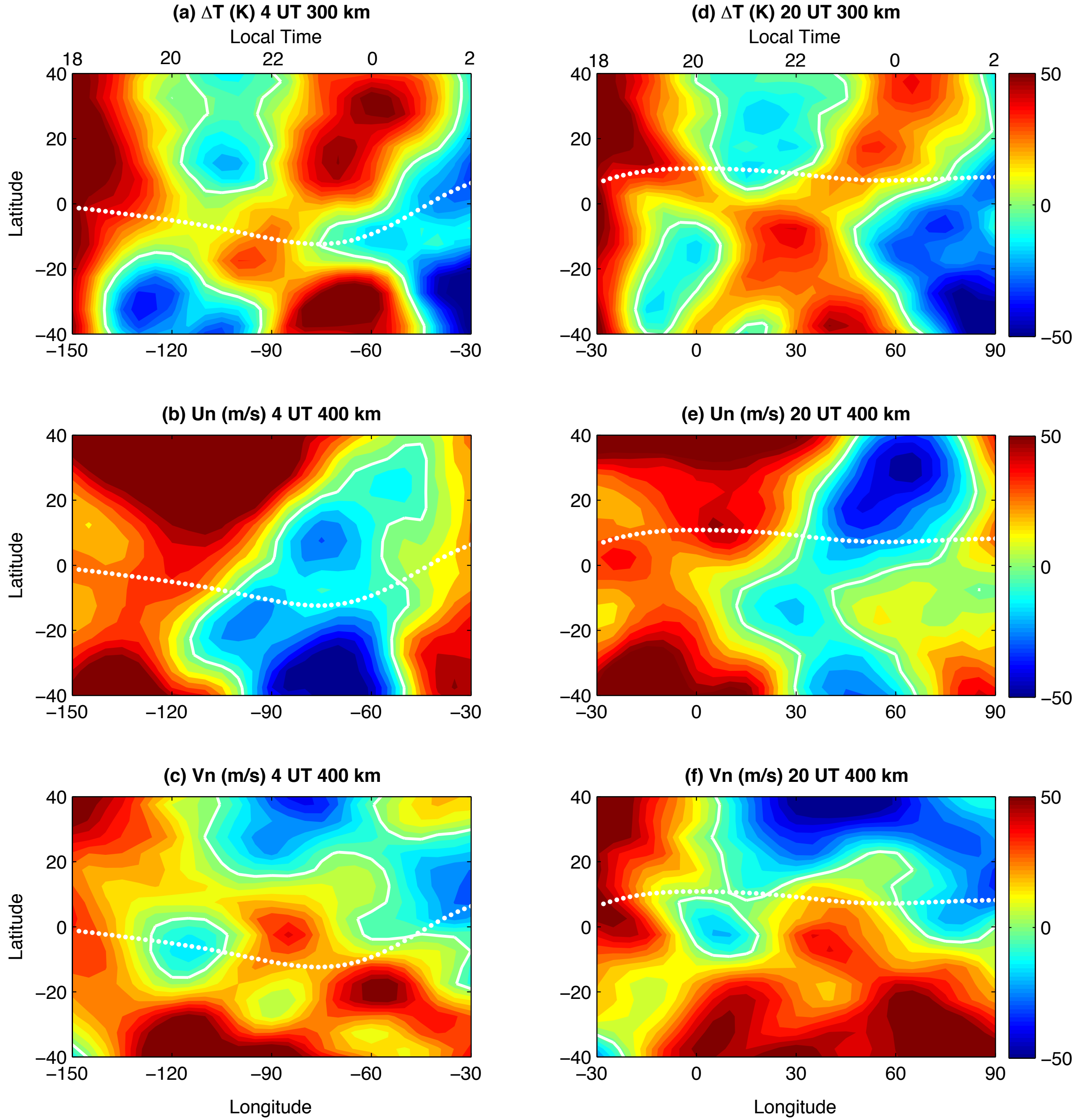

(a) ΔT (K) 4 UT 300 km
Local Time
(d) ΔT (K) 20 UT 300 km
Local Time
(b) Un (m/s) 4 UT 400 km
(e) Un (m/s) 20 UT 400 km
(c) Vn (m/s) 4 UT 400 km
(f) Vn (m/s) 20 UT 400 km
Latitude
Longitude

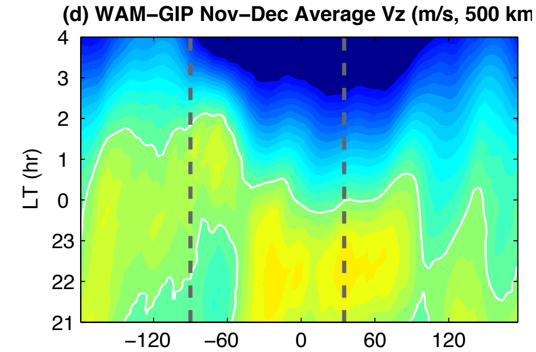

(d) WAM–GIP Nov–Dec Average Vz (m/s, 500 km
LT (hr)

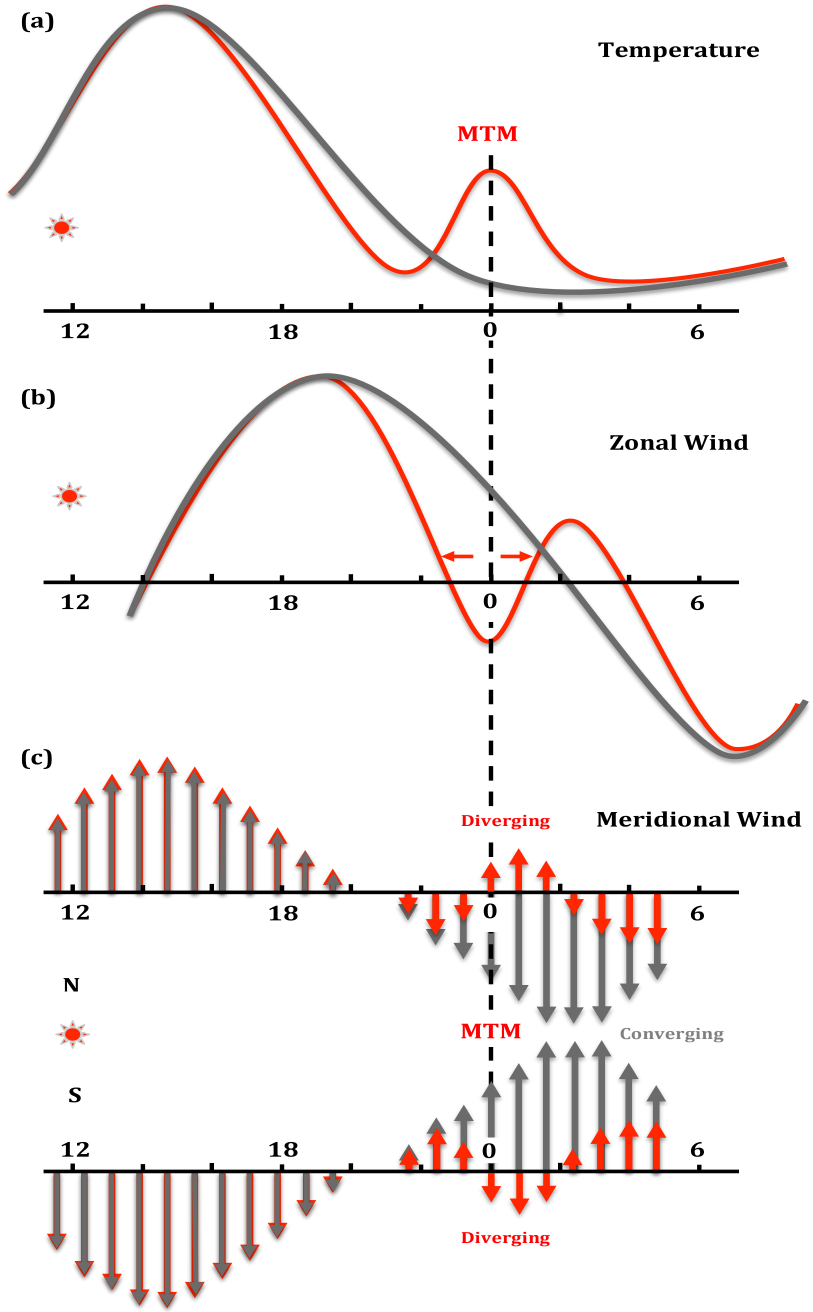
(a)
Temperature
MTM
12
18
0
6
(b)
Zonal Wind
12
18
0
6
(c)
Meridional Wind
Diverging
12
18
0
6
N
MTM
Converging
S
12
18
0
6
Diverging

Nighttime Wind Dynamo Test

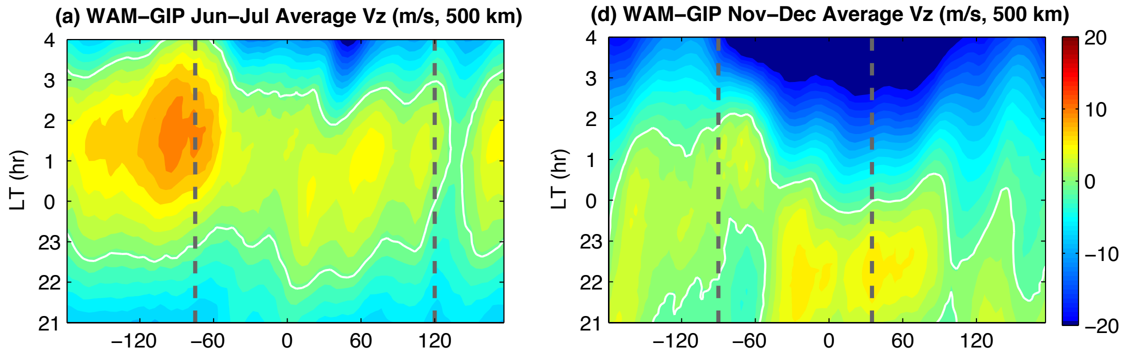

Two-month average

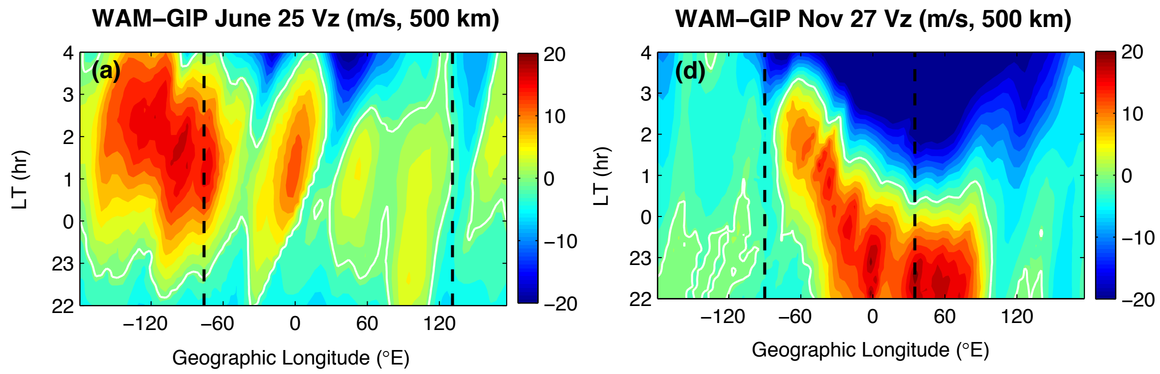

One-day

Nighttime Wind Dynamo Test

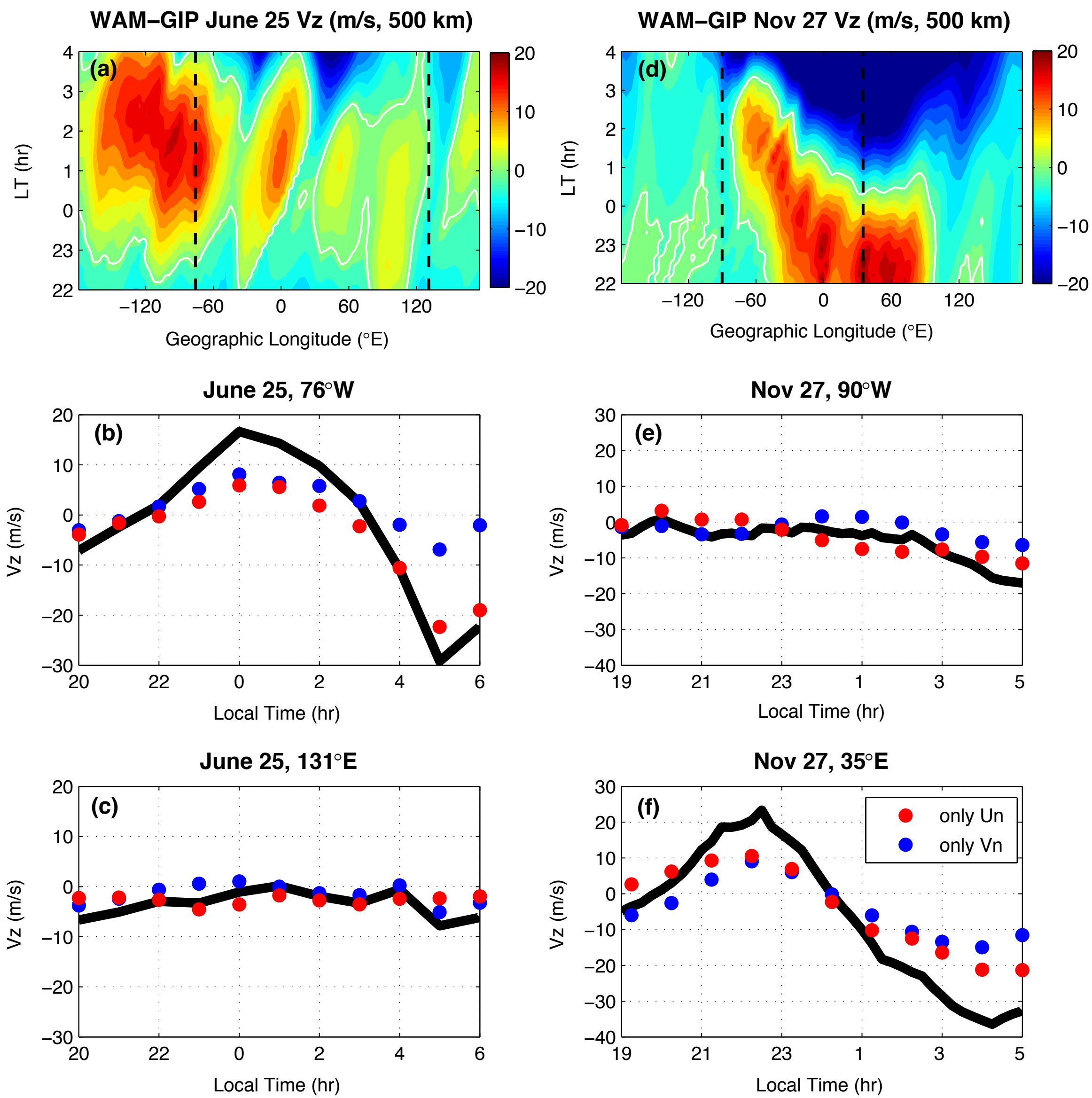

- Both winds are important in forming the post-midnight upward drift. The large downward drift near dawn is largely created by the zonal wind.
- The contribution of winds to the post-midnight vertical drift can be different at different longitudes.

Conclusion

- The coupled WAM-GIP model is capable of simulating the impact of MTM on the nighttime thermosphere and ionosphere system.
- The upward equatorial vertical drifts occurring during the post-midnight period are strongly associated with the wind changes due to the MTM in the nighttime thermosphere.
- The MTM locally reverses the typical large-scale zonal and meridional wind pattern, in turn affecting the nighttime *F*-layer electrodynamics. Causal mechanisms of post-midnight upward drift can be partially explained by those lead to the pre-reversal enhancement during post-sunset period [*Richmond et al*., 2014].
- The longitudinal variation of the drifts depends on the magnitude and position of the MTM peak relative to the magnetic equator. Both zonal and meridional wind contribute to the post-midnight upward drift.
- Other nighttime ionospheric phenomena that are associated with the MTM, such as midnight collapse, brightness waves, nighttime TEC enhancement, and post-midnight irregularities, will also be simulated and investigated through the theoretical models in the future.

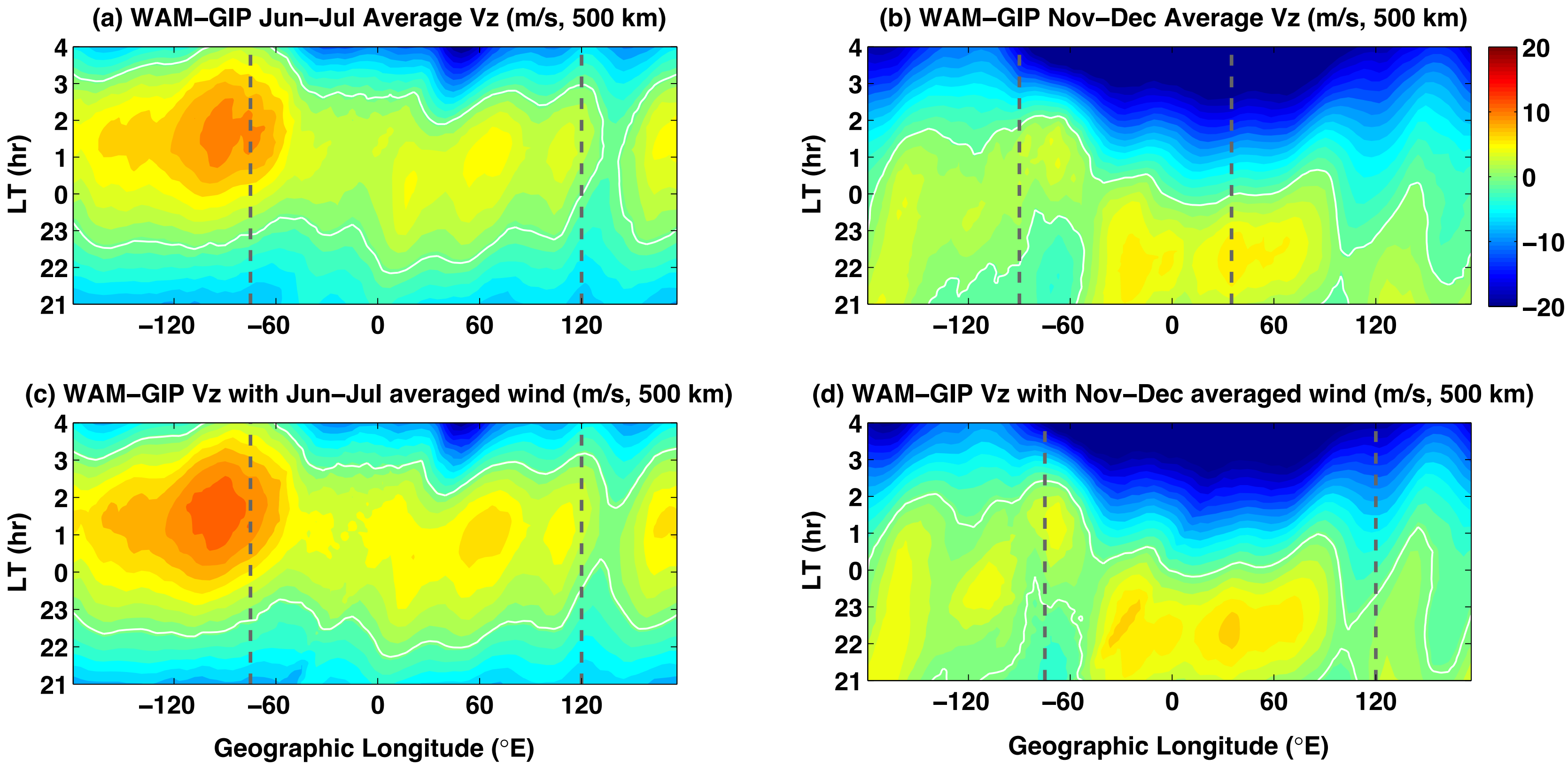

(a) WAM–GIP Jun–Jul Average Vz (m/s, 500 km)
(b) WAM–GIP Nov–Dec Average Vz (m/s, 500 km)
(c) WAM–GIP Vz with Jun–Jul averaged wind (m/s, 500 km)
(d) WAM–GIP Vz with Nov–Dec averaged wind (m/s, 500 km)
LT (hr)
4
3
2
1
0
23
22
21
–120
–60
0
60
120
20
10
0
–10
–20
Geographic Longitude (°E)

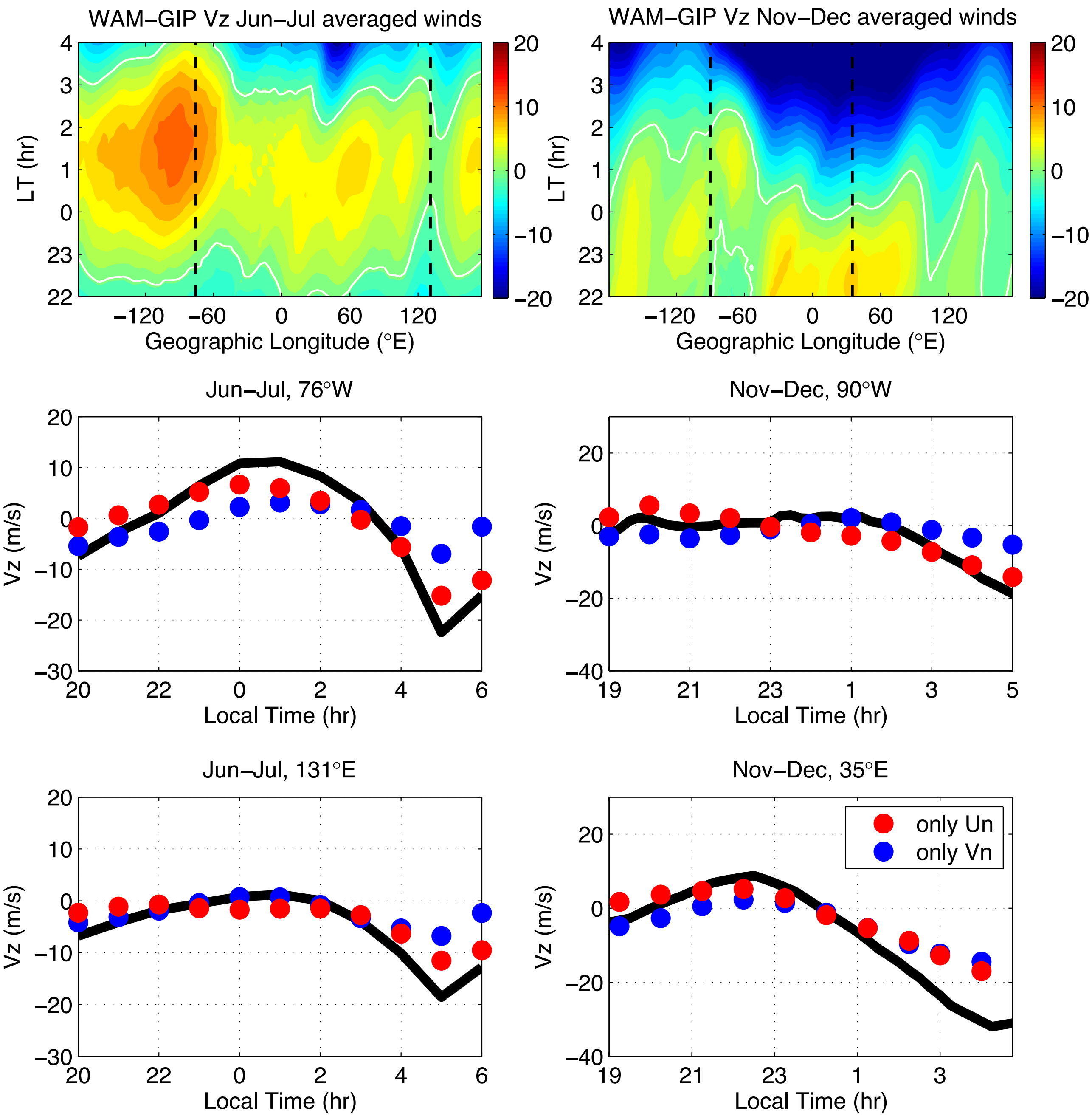
WAM−GIP Vz Jun−Jul averaged winds
LT (hr)
Geographic Longitude (°E)
WAM−GIP Vz Nov−Dec averaged winds
Jun−Jul, 76°W
Nov−Dec, 90°W
Jun−Jul, 131°E
Nov−Dec, 35°E
Vz (m/s)
Local Time (hr)
only Un
only Vn